

Necessarily transient quantum refrigerator

Sreetama Das, Avijit Misra, Amit Kumar Pal, Aditi Sen(De), and Ujjwal Sen
Harish-Chandra Research Institute, Chhatnag Road, Jhansi, Allahabad - 211019, India

We show that one can construct a quantum absorption refrigerator that provides refrigeration only in the transient regime, by using three interacting qubits, each of which is also interacting with local heat-bath. The machine either does not provide cooling in the steady state, or the steady state is achieved after a long time. We propose a canonical form of qubit-bath interaction parameters that generates transient cooling without steady-state cooling, and claim that such a phenomenon is generic to small-scale quantum absorption refrigerators. We also show that it is generically possible to have fast cooling. We demonstrate our results for two separate models of thermalization, and show that a transient cooling without steady-state cooling is associated with generation of negligible, or no bipartite quantum correlations. For one of the models of thermalization, we find that the minimum achievable temperature of the refrigerated qubit can remain almost frozen, i.e., unchanged, for a significant region of the parameter space.

I. INTRODUCTION

Study of the thermodynamic properties of microscopic quantum systems has been an active field of research in recent times [1–7]. Considerable efforts have been directed to develop and characterize quantum heat engines, and to determine whether “quantum” advantages can be obtained in these machines over their classical counterparts [8]. Quantum analogues of the well-known classical Carnot and Otto engines have been extensively studied [9–13], and implemented in laboratories using mesoscopic substrates [14], superconducting qubits [15], quantum dots [16], and ionic systems [17].

On one hand, this has motivated researchers to test the laws of thermodynamics at the quantum mechanical level [7, 18], and to determine the efficiencies of quantum heat engines, analogous to those provided by the enormously studied classical heat engines [19]. On the other hand, a great deal of interest has been attracted towards building “small” quantum refrigerators, which consist of only a few quantum levels, and the energy required to drive the refrigerator is obtained from local heat baths attached to the subsystems constituting the refrigerator, known as the absorption refrigerator [20–26]. Despite their simple working principles, small quantum refrigerators are shown to be useful in quantum error correction, where cold ancillary qubits are considered as resources [27]. Implementation schemes for such models in laboratories [28] have also been proposed. The motivation for studying such microscopic refrigerators from an information-theoretic perspective [26] lies, for example, in the facts that thermodynamics has a close connection with both classical and quantum information theory [29].

A special phenomenon, namely, the “steady-state cooling”, in the case of a quantum self-sufficient refrigerator constituted of only three qubits [20–26] has recently been in focus. Here, the steady state temperature of one of the qubits, called the “cold” qubit, is less than its initial temperature, and it, in general, can occur at large time in the dynamics. However, refrigeration at short time in these models, which can be more accessible in the experiments, remains a relatively less explored topic. Only recently a few studies have addressed this issue [24, 26], and pointed out the benefit of transient cooling over the steady state cooling, by using uncorrelated product thermal

states as well as states with coherence in the energy eigenbasis, as the initial states. It has been shown that the transient regime of such refrigerators may provide a better cooling, in the sense of attaining a lower temperature, as compared to that in its steady state, which highlights the importance of the study of the systems as it approaches towards its equilibrium. In situations where the time scale to attain the equilibrium is too high to implement, or where very fast cooling is required, transient cooling may emerge as the *practical* option to attain refrigeration. In this paper, we ask the following question: Can there exist a situation where the transient cooling is the only option for refrigeration to occur? In this scenario, no steady-state cooling takes place. The next immediate question is to find out whether such a phenomenon is generic to small quantum refrigerators irrespective of the different models of thermalization. This paper answers both the questions affirmatively.

Towards this aim, we consider two paradigmatic models of thermalization for a three-qubit self-contained quantum refrigerator attached to local heat baths. One of them is the well-studied reset model [21], and the other one is a more realistic scenario where the local baths are collection of harmonic oscillators that interact with the qubits via memoryless interactions [26]. We identify a *canonical* form of the qubit-bath interaction parameters which eases the presentation of situations where no steady-state cooling takes place, and transient cooling is the only option to attain refrigeration. We demonstrate this phenomenon for both the models, and find out regions in the space of the qubit-bath parameters where such a phenomenon takes place. Also, we point out that with a slight modification of our canonical form of the qubit-bath interactions, a condition emerges where the system cools fast and attains its minimum temperature either at the steady state, or in the transient regime. For each set of parameters, we quantify the speed of cooling by introducing a “half-time”, which the system takes to attain half the maximum cooling possible for the fixed set of parameters. Our result indicates that such a situation is generic to the different models of thermalization for the three-qubit quantum absorption refrigerator. Moreover, we show that in the parameter space where transient cooling is the only option for refrigeration, negligible or no bipartite quantum correlations in all the possible bipartitions of the three-qubit system is generated during the initial phase of the dynamics. Interestingly, for

the model of thermalization involving collections of harmonic oscillators as local bath, a “freezing”, i.e., almost invariance, of the minimum temperature attained of the cold qubit with respect to change in system parameters is observed.

The paper is organized as follows. In Sec. II, we discuss the necessarily transient self-contained three-qubit quantum absorption refrigerator with two specific models of thermalization. While Sec. II A deals with the reset model of thermalization, a more realistic model with local heat-baths constituted of harmonic oscillators is presented in Sec. II B. In Sec. III, we discuss the properties of bipartite quantum correlations in the system of three-qubits under the qubit-bath interactions corresponding to both the models discussed in this paper. Sec. IV contains the concluding remarks.

II. THREE-QUBIT QUANTUM ABSORPTION REFRIGERATOR

We consider a quantum absorption refrigerator consisting of three qubits [20, 24] labeled “1”, “2”, and “3”. The first qubit, “1”, represents the qubit which is to be cooled, while “2” and “3” behave as the refrigerator. The ground and excited states of the systems are given by $|0\rangle_i$ and $|1\rangle_i$, respectively, where $i \in \{1, 2, 3\}$. Describing the qubits in terms of standard Pauli representations, $\sigma_i^{x,y,z}$, where $\{|0\rangle, |1\rangle\}$, the eigenvectors of σ^z , forms the computational basis, the free Hamiltonian of the three-qubit system can be written as

$$\tilde{H}_{loc} = \frac{k}{2} \sum_{i=1}^3 E_i \sigma_i^z, \quad (1)$$

where the ground and excited state energies of the qubit i are given by $-\frac{E_i}{2}$ and $\frac{E_i}{2}$, respectively, and k is a constant having the dimension of energy. The coupling between the qubits is represented by a three-body interaction Hamiltonian,

$$\tilde{H}_{int} = kg(|010\rangle\langle 101| + h.c.), \quad (2)$$

with kg being the corresponding interaction strength. Each of the qubits is considered to be weakly interacting with a heat bath of temperature \tilde{T}_i , where $\tilde{T}_1 \leq \tilde{T}_2 < \tilde{T}_3$. The third qubit is coupled with the hottest bath, while the bath associated with the second qubit is considered to be at room temperature. We assume that the interactions between the qubits are switched on at time $\tilde{t} = 0$, such that $kg \geq 0$ for $\tilde{t} > 0$. All the qubits are initially in a thermal equilibrium state with their respective baths, and the initial state of the three-qubit system is given by $\rho_0 = \rho_0^1 \otimes \rho_0^2 \otimes \rho_0^3$, with

$$\rho_0^i = \frac{1}{Z_i} \exp(-\tilde{\beta}_i k E_i \sigma_i^z / 2). \quad (3)$$

Here, $Z_i = \text{Tr} [\exp(-\tilde{\beta}_i k E_i \sigma_i^z / 2)]$ is the partition function corresponding to the qubit i , and $\beta_i = (k_B \tilde{T}_i)^{-1}$, k_B being the Boltzmann constant.

The dynamics of the entire three-qubit system, controlled by the choice of the system parameters as well as the parameters corresponding to the system-bath interaction, drives the system

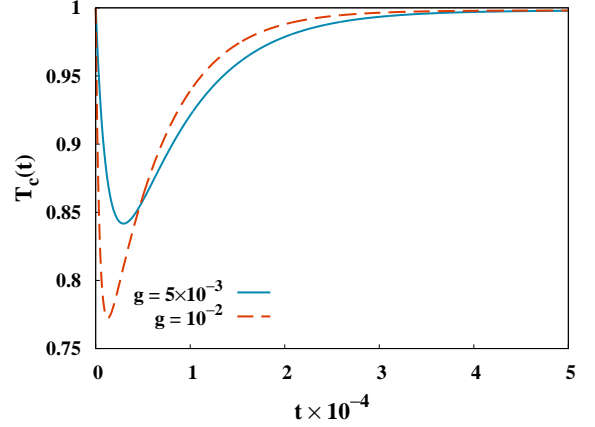


Figure 1. (Color online) Necessarily transient reset model refrigerator. We show here the behaviour of cold-qubit temperature with time. We plot the variation of $T_c(t)$ as a function of t . We set $g = 5 \times 10^{-3}$ (continuous line) and 10^{-2} (dashed line). We choose $x = 3.5$ and $y = 2.5$, with $p_1 = 10^{-3.5}$, $p_2 = 10^{-6}$, $p_3 = 10^{-1}$. All quantities are dimensionless.

to a time-evolved state $\rho(t)$, which is obtained as a solution of the master equation

$$\frac{\partial \rho}{\partial t} = -\frac{i}{\hbar} [\tilde{H}_{loc} + \tilde{H}_{int}, \rho] + \Phi(\rho). \quad (4)$$

Eq. (4) governs the dynamics of the three-qubit system, where the operator Φ depends solely on the type of the local reservoirs attached to the qubits, and the type of interaction between the qubits and the reservoirs. Let us now re-write the dynamical equation in dimensionless variables and parameters as

$$\frac{\partial \rho}{\partial t} = -i[H_{loc} + H_{int}, \rho] + \frac{\hbar}{k} \Phi(\rho), \quad (5)$$

where $t = k\tilde{t}/\hbar$, $H_{loc} = \tilde{H}_{loc}/k$, and $H_{int} = \tilde{H}_{int}/k$. The second term on the right-hand-side will be written in dimensionless form after an explicit definition of $\Phi(\rho)$, to be given later. Let us also introduce the dimensionless parameter $T = k_B/k$ times the absolute temperature, so that the initial state of the i th qubit is

$$\rho_0^i = \frac{1}{Z_i} \exp(-E_i \sigma_i^z / 2T_i). \quad (6)$$

The transient temperature, $T_c(t)$, of the cold qubit (i.e., the qubit to be cooled, which is qubit “1”) is determined by using Eq. (3), from the local density matrix $\rho^1(t)$ corresponding to the cold qubit, obtained by tracing out qubits 2 and 3 from $\rho(t)$. Note here that $T_c(t)$ is a function of the system parameters and the parameters corresponding to the qubit-bath interactions also. If $T_c(t) < T_1$ at some specific value of t , we call it to be a successful cooling of the qubit “1” with the help of the refrigerator, i.e., qubits “2” and “3”. Let us denote the steady state temperature of the cold qubit by T_1^s , which corresponds to the steady state of the system, given by $\partial \rho / \partial t = 0$. We call a situation to be of steady state cooling (SSC) if $T_1^s < T_1$, while

$T_c(t) < T_1$ represents a case of transient cooling (TC) at time t .

We now discuss the occurrence of SSC and TC in two different scenarios. The scenarios differ by the choices of the heat baths and the types of qubit-bath interactions. Unless otherwise mentioned, in both the cases, we consider $E_1 = 1$, and $T_1 = 1$. We take $T_2 = T_1$, implying a scenario where the cold qubit is initially at room temperature, like the second qubit. We further set $E_2 = E_1 + E_3$. Note here that $[H_{loc}, H_{int}] = 0$, so that in the closed evolution, the interaction and the field energies are separately conserved. Note that the initial state, ρ_0 , is diagonal in the eigenbasis of H_{loc} , and the only off-diagonal elements emerging in the evolved state due to H_{int} are $|010\rangle\langle 101|$ and its hermitian conjugate. The qubit-bath interactions do not generate coherence between the eigenbasis elements of the individual qubits, thereby keeping the form of $\rho(t)$ unchanged. Thus, it leads to diagonal local density matrices corresponding to each qubit, obtained by tracing out the other two qubits from $\rho(t)$. This allows one to define a local temperature for the cold qubit at every time instant t , according to Eq. (3).

A. Reset model

The first example that we consider deals with the representation of the qubit-bath interaction via a simple “reset model” [21], where at every time step, a probabilistic *reset* occurs to the state of each of the three qubits. With a high probability, the state of qubit i is left unchanged, while in the rest of the situations, the qubit is reset to the initial thermal state ρ_0^i . Hence the operator Φ , in this case, is given by

$$\Phi(\rho) = \sum_{i=1}^3 \tilde{p}_i(\varphi_i(\rho) - \rho), \quad (7)$$

where $\{\tilde{p}_i\}$ are the probability densities per unit time, and $\varphi_i(\rho) = \rho_0^i \otimes \text{Tr}_i(\rho(t))$. We now introduce the dimensionless parameter, $p_i = \frac{\hbar}{k} \tilde{p}_i$, thus resulting in a dimensionless second term in the dynamical equation (5). For such a qubit-bath interaction, the master equation given in Eq. (5) can be applied in the perturbative regime, where $g, p_i \ll E_1, E_3$ [21]. Following the methodology discussed in [20, 24], for fixed values of the system parameters, the steady state temperature of the cold qubit and the transient temperature as a function of time can be computed. It has been observed that for $g > p_i, i \in \{1, 2, 3\}$, $T_c(t)$ initially oscillates with an approximate frequency g/π , until dissipation dominates and the system approaches to its steady state [24]. Typically, the time taken (in units of the dimensionless parameter, t) for the dissipative dynamics to damp out the oscillations was found to scale as q where $q^{-1} = \sum p_i$. For specific values of the probabilities, $\{p_i\}$, it has been shown that the temperature of the cold qubit in the transient regime can be lower than that of the steady state, i.e., one can have situations for which $T_c(t) < T_1^s$. This implies that the refrigerator can be more effective in the transient domain compared to being in the steady state. In this paper, we wish to find out the parameter region in which TC occurs without any

SSC. Specifically, we are now interested in the scenario where $T_c(t) < T_1^s = T_1$.

Canonical qubit-bath interaction parameters. We propose a *canonical* form of a set of qubit-bath interaction parameters, $\{\kappa_i\}$, as

$$\kappa_1 = 10^{-x}, \quad \kappa_2 = 10^{-(x+y)}, \quad \kappa_3 = 10^{-(x-y)}, \quad (8)$$

where $x, y \geq 0$, such that $\max\{\kappa_1, \kappa_2, \kappa_3\} = \kappa_3$, and $\kappa_i \leq 1$. We refer to the choice of the parameters according to Eq. (8) as the canonical qubit-bath interaction parameters (CIP). The proper choices of x and y dictates the values of $\{\kappa_i\}$. For example, the dimensionless qubit-bath interaction parameters $\{p_i\}$ in the reset model can be chosen according to Eq. (8). We shall show that such a choice of $\{p_i\}$ will finally lead to the TC without the SSC. However, the choice of the values of x and y have to be made in such a way that the master equation remains valid. We will see later that such choice of these parameters can be useful in other models also, discussed in the succeeding subsection.

Refrigeration in a necessarily transient regime. We demonstrate the usefulness of CIP in characterizing the necessarily transient three-qubit quantum absorption refrigerator in the case of the present model. This corresponds to a scenario where the qubit-bath coupling corresponding to the hot qubit is the strongest, while that of the intermediate qubit is the weakest. Since the intermediate qubit is the one dissipating energy into the environment, a weak coupling of this qubit with the heat-bath may lead to a high steady-state temperature, while transient cooling can still be achieved in this regime.

Let us consider $x = 3.5$ and $y = 2.5$, such that $p_3 = 10^{-1}$, and $p_2 < p_1, p_3$. The rest of the system parameters are set at $E_3 = 10^2$ and $T_3 = 10^2$. The variation of $T_c(t)$ as a function of t for different values of g ($g = 5 \times 10^{-3}$ (continuous graph) and 10^{-2} (dashed graph)) are shown in Fig. 1. The temperature of the cold qubit (qubit “1”) decreases at first, reaches a minimum, and then increases to attain a steady state at a temperature $T_1^s \approx T_1$, i.e., the steady state temperature is approximately the same as the initial temperature, for the cold qubit. Such phenomena can be observed by tuning the system parameters and the qubit-bath interaction parameters, as shown in Fig. 1. It is clear that in scenarios like this, cooling in the steady state is negligible, while substantial cooling occurs in the transient regime. Therefore, the three-qubit system represents a *necessarily* transient quantum absorption refrigerator, since the only way of obtaining the cold qubit at a temperature lower than T_1 is to halt the dynamics at a time t in the transient regime, i.e., when $T_c(t) < T_1$. In other words, there exist points in the parameter space, where, if the experimentalist finds herself/himself forced to work in, due to may be some practical limitations in the laboratory technology, the only way to have a refrigerator, within the reset model, is to consider a transient regime cold qubit.

Next, we establish that there exists substantial regions in the space of $\{p_i\}$, where TC is the only option to obtain refrigeration. In Fig. 2, we plot T_1^s, δ, T_{min} , and t_{min} as functions of x and y for fixed values of g , viz. $g = 10^{-3}$ and $g = 10^{-2}$. Here, $T_{min} = \min_t T_c(t)$, t_{min} is the time at which this minimization

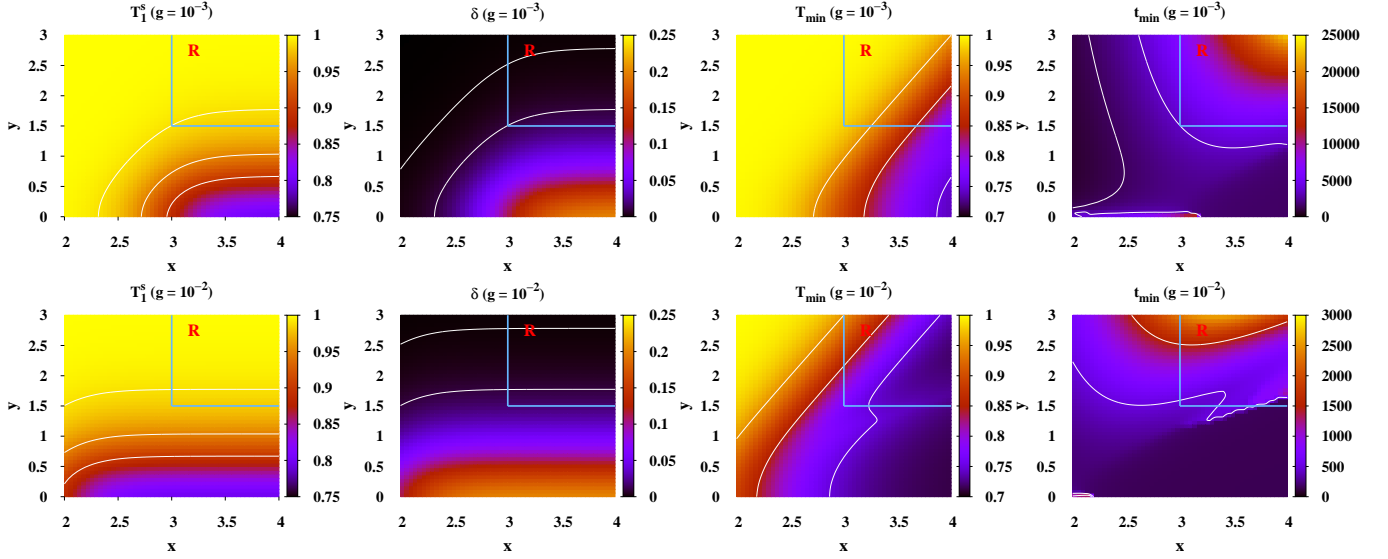


Figure 2. (Color online) Thermodynamic system characteristics in the reset model on the CIP plane. We present the projection-plots of (from left to right) T_1^s , $\delta = T_1 - T_1^s$, T_{min} , and t_{min} as functions of x (horizontal axis) and y (vertical axis). We choose $g = 10^{-3}$ (first row) and $g = 10^{-2}$ (second row). The thin lines correspond to $T^s = 0.9, 0.95, 0.99$ (from bottom to top), $\delta = 0.01, 0.001$ (from bottom to top), $T_{min} = 0.75, 0.85, 0.95$ (from right to left), $t_{min} = 1500, 3500$ (from bottom to top, in the case of t_{min} , with $g = 10^{-3}$, the left most line corresponding to 1500), and $t_{min} = 500, 1500$ (from bottom to top, with $g = 10^{-2}$). The first quadrants of the figures, where the copious occurrences of TC without SSC is found, are marked by “R” and bounded by the thick continuous lines. All quantities are dimensionless.

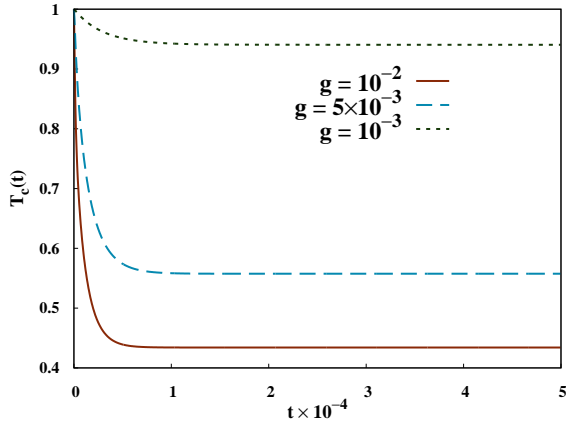


Figure 3. (Color online) Fast and steady cooling in the reset model. We plot the variation of $T_c(t)$ versus t . We choose $x = 2.5$, $y = 1$, and $g = 10^{-3}$ (short-dashed line), 5×10^{-3} (dashed line) and 10^{-2} (continuous line), with $p_1 = 10^{-2.5}$, $p_2 = 10^{-3.5}$, $p_3 = 10^{-1.5}$. All quantities are dimensionless.

occurs, and

$$\delta = T_1 - T_1^s. \quad (9)$$

To perform the minimization as well as for obtaining a typical dynamics profile, we always focus on the range $0 \leq t \leq 5 \times 10^4$. In this section, and in all the subsequent discussions, we consider $t = 5 \times 10^4$ to be large time. We find that at all the points considered on the (x, y) plane, bounded by the regions

$2 \leq x \leq 4$, and $0 \leq y \leq 3$, the temperature of the cold qubit almost reaches the steady state temperature at $t = 5 \times 10^4$. The thin lines on the plots refer to the lines corresponding to fixed values of the relevant quantities, as mentioned in the caption of Fig. 2. We observe that there exist regions on the (x, y) plane, where $\delta < 10^{-2}$, implying a negligible or no steady state cooling, and so in these regions, transient cooling is the only plausible alternative. Indeed, we find that in these regions, T_{min} has a sufficiently low value compared to the initial temperature of the cold qubit, T_1 . This situation is “rich” in the first quadrant of the region considered over the (x, y) plane, which we mark by “R”, and enclose by the thick continuous lines, which include the regions where the system provides a refrigeration that is necessarily transient. With increasing values of g , the region expands, as is clearly observed by comparing the data with $g = 10^{-2}$ and $g = 10^{-3}$. Note also that the coldest temperature for the cold qubit in the transient regime is attained faster if the value of g is increased. This can be understood from the lower values of t_{min} corresponding to $g = 10^{-2}$, compared to those corresponding to $g = 10^{-3}$. Note however that δ is positive over the entire region of the (x, y) plane considered, which implies that no steady state heating has taken place in this parameter space. We will see in the next subsection that this is not the case when a different thermal bath is considered.

Fast and steady cooling. Let us now study a situation where we relax the condition $T_1^s \approx T_1$. We are now interested to change CIP in such a way that an occurrence of SSC can take place, which can be along with TC, i.e., $T_1^s, T_c(t) < T_1$. Moreover, we claim that such cooling process should happen with very short time scale, t . Such phenomena emerges by interchanging κ_1 and κ_2 , which, following Eq. (8), leads to

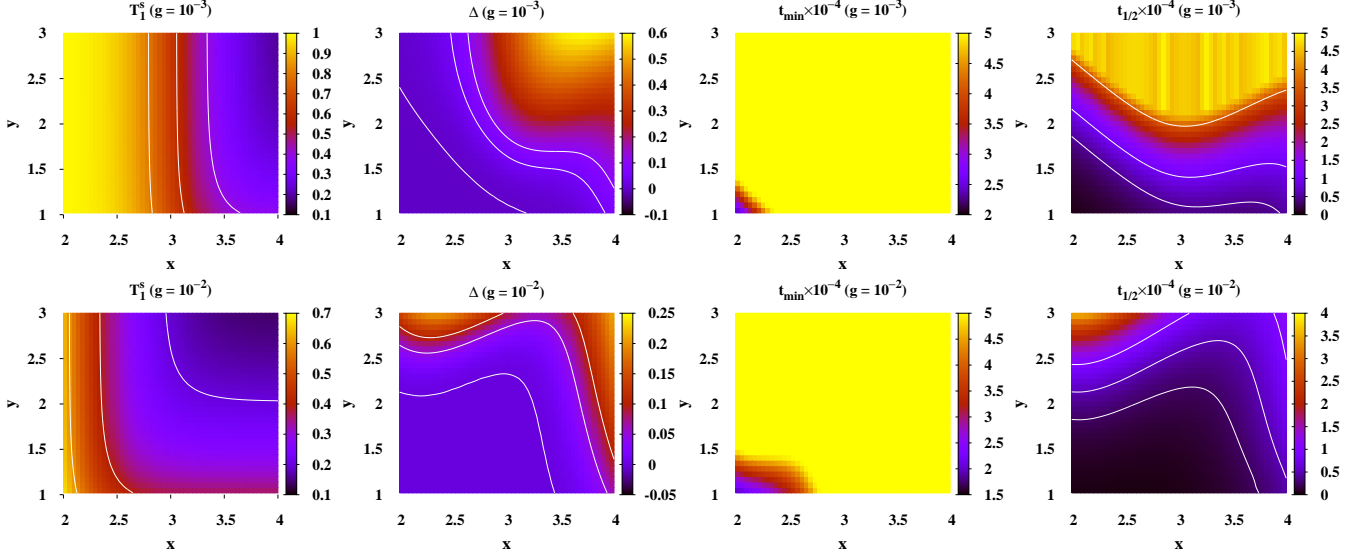


Figure 4. (Color online) Thermodynamic system characteristics in the reset model on the CIP plane when the steady state is relatively far off in time. We plot the variations of T_1^s , $\Delta = T_{\min} - T_1^s$, t_{\min} , and $t_{1/2}$ with x and y . We set $g = 10^{-3}$ (top row) and $g = 10^{-2}$ (bottom row). The thin lines in the figures correspond to $T_1^s = 0.4, 0.6, 0.8$ (from right to left, $g = 10^{-3}$), $T_1^s = 0.2, 0.4, 0.6$ (from right to left, $g = 10^{-2}$), $\Delta = 10^{-3}, 0.05, 0.1$ (from bottom to top, for both $g = 10^{-3}$ and 10^{-2}), $t_{1/2} = 0.5, 1, 3.5$ (from bottom to top, $g = 10^{-3}$), and $t_{1/2} = 0.25, 0.5, 1$ (from bottom to top, $g = 10^{-2}$). All quantities are dimensionless.

$\kappa_1 \leq \kappa_2$. As an example, we consider the case of $x = 2.5$ and $y = 1$, such that $p_1 = 10^{-2.5}$, $p_2 = 10^{-3.5}$, and $p_3 = 10^{-1.5}$, for which the variation of $T_c(t)$ is depicted in Fig. 3 for $g = 10^{-3}$, 5×10^{-3} , and 10^{-2} . The temperature of the cold qubit decreases rapidly with time, and becomes steady at a temperature much lower than its initial temperature, given by $\min_t T_c(t)$. Note here that because of the damped coherence dynamics and the gradual approach of the temperature of the cold qubit towards its steady state, faster cooling can be achieved without precise time control. The value of T_1^s is found to increase with decreasing g . Moreover, note that for these parameter values, unlike previous studies in [24], $T_c(t)$ does not show any oscillation with t .

Let us introduce the quantity $\delta_c = T_1 - T_1^s$, which quantifies the maximum cooling that is obtained in the scenario. We define the “half-time”, $t_{1/2}$, as the time at which $T_c(t) = T_1 - \frac{\delta_c}{2}$. In the case of the damped coherence dynamics, the half-time provides a measure of how fast the temperature of the cold qubit approaches its minimum value, which is the steady state temperature. The lower the value of $t_{1/2}$, the faster is the approach of the cold qubit to its steady state. However, even when the coherence dynamics is not damped, a lower value of $t_{1/2}$ indicates that there is a possibility of significantly fast cooling of the cold qubit before it reaches its steady state.

As in the previous case, we investigate whether this phenomenon occurs in a considerable region of the parameter space. In order to do so, we focus on the region $2 \leq x \leq 4$ and $1 \leq y \leq 3$ over the (x, y) - plane. Fig. 4 depicts the variations of T_1^s , $\Delta = T_{\min} - T_1^s$, t_{\min} , and $t_{1/2}$ as functions of x and y for different values of g . Note that in contrast to the previous case of transient refrigeration, substantial

steady state cooling takes place in the present situation, as can be clearly understood from the range of the values of T_1^s . Similar to the previous case of transient refrigeration, we determine $T_{\min} = \min_t T_c(t)$ in the range $0 \leq t \leq 5 \times 10^4$. Note that both positive and negative values of $\Delta = T_{\min} - T_1^s$ occurs in this region, as seen in the second column in Fig. 4. For our choice of parameters, we can observe two different scenarios. **Case 1.** When $\Delta > 0$, i.e., when TC occurs, we find that the steady state is not reached up to $t = 5 \times 10^4$, which is indeed the case for most of the values of x and y , as seen from the third column of Fig. 4. Here, $t_{\min} = 5 \times 10^4$ indicates that the steady state is yet to be reached. This is another parameter space where TC is again beneficial. **Case 2.** For $\Delta < 0$, i.e., when SSC takes place, we notice that there exists regions in which $t_{\min} < 5 \times 10^4$. We infer that region as a useful parameter space for fast steady state cooling. Moreover, we find that the region increases with the increase of g .

Note. For the purpose of demonstration, we plot in Fig. 1 only those dynamics profiles where no initial oscillation of $T_c(t)$ takes place. However, initial oscillation of $T_c(t)$ is indeed possible from the CIP, depending on the values of g and $\{p_i\}$. In most of the cases corresponding to CIP, damped coherence dynamics is observed when one approaches steady state cooling (eg. Fig. 3), which implies a faster cooling without precise time control.

B. Thermalization by memoryless qubit-bath interaction

Let us now move to a more realistic scenario, under the standard Born-Markov assumption of a memoryless system-bath

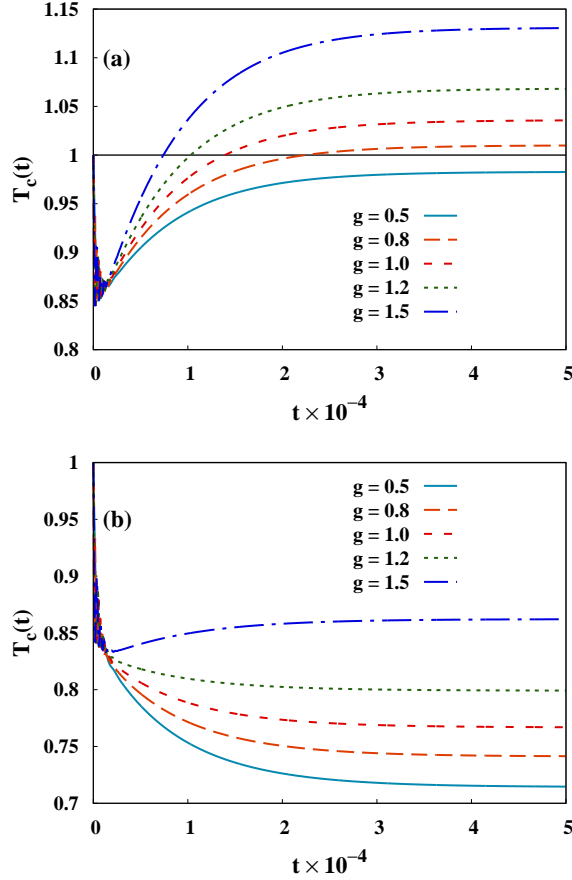


Figure 5. (Color online) Necessarily transient refrigerator for thermalization with collections of harmonic oscillators as local heat baths. We plot $T_c(t)$ against t . We choose $x = 4$ and $y = 1$. Two different scenarios, namely, (a) $\alpha_1 = 10^{-4}$, $\alpha_2 = 10^{-5}$, $\alpha_3 = 10^{-3}$, and (b) $\alpha_1 = 10^{-5}$, $\alpha_2 = 10^{-4}$, $\alpha_3 = 10^{-3}$ are considered for $0.5 \leq g \leq 1.5$.

interaction. Our aim is again to find out a range of parameters which can be tuned in such a way that the refrigeration occurs only in the transient regime. The dynamics of this model is governed by a quantum master equation of the Lindblad form, given in Eq. (4). The difference of this model from the previous one lies in the choice of the bath. In this case, each qubit is coupled to a bath constituted of an infinite set of harmonic oscillators having a broad range of frequencies, ω . The total Hamiltonian of the bath is given by $\tilde{H}_b = \sum_{i=1}^3 \hbar \nu_{i,k} b_{i,k}^\dagger b_{i,k}$, where we assume the baths to be spatially well separated to neglect any interaction between them. Here, $\nu_{i,k}$ is the frequency of the mode k of the bath i , and the b 's are the bosonic mode operators. The interaction Hamiltonian between the qubits and the baths is given by $\tilde{H}_{sb} = \sum_{i=1}^3 \mathcal{A}_i \otimes \mathcal{X}_i$, where $\mathcal{A}_i = \sigma_i^x$ are the Lindblad operators responsible for transitions between different eigenstates of the fully-coupled Hamiltonian $\tilde{H}_{loc} + \tilde{H}_{int}$, and $\mathcal{X}_i = \sum_{k=1}^{\infty} (\eta_{i,k} b_{i,k} + \eta_{i,k}^* b_{i,k}^\dagger)$ are the collective bath coordinates. Here, the subscript “sb” stands for “system-bath”,

and the strength of the qubit-bath couplings are denoted by $\eta_{i,k}$. The Hamiltonian describing the system consisting of the three qubits and their respective baths is then given by $\tilde{H}_{tot} = \tilde{H}_{loc} + \tilde{H}_{int} + \tilde{H}_b + \tilde{H}_{sb}$. We assume that the spectral function corresponding to the bath i is of the form of an Ohmic spectral function, given by $\tilde{J}_i(\omega) = \alpha_i \omega \exp(-\omega/\Omega)$ where α_i is the dimension-less coupling strength defining the qubit-bath coupling, and Ω is the “cut-off frequency”, such that the memory time of the baths $\sim \Omega^{-1}$. Since we are interested in the Markovian dynamics, Ω must be much larger than a typical frequency ω , while $\alpha_i \ll 1$ [26].

We now consider the specific case of this thermalization model, where the dissipation rates are much smaller than the coupling strength, g . Following [26], one can derive the Markovian master equation for the three-qubit system in this model described above. Here, the operation Φ in the master equation is given by

$$\Phi(\rho) = \sum_{i,\omega} \tilde{\gamma}_i(\omega) \varphi_i^\omega(\rho), \quad (10)$$

where $\{\tilde{\gamma}_i(\omega)\}$ represents the incoherent transition rates between the eigenstates of the Hamiltonian $\tilde{H}_{loc} + \tilde{H}_{int}$. In terms of the spectral functions of each bath, $\tilde{\gamma}_i(\omega)$ can be obtained as [26]

$$\tilde{\gamma}_i(\omega) = \begin{cases} \tilde{J}_i(\omega) \{1 + f(\omega, \tilde{\beta}_i)\}, & (\omega > 0) \\ \tilde{J}_i(|\omega|) f(|\omega|, \tilde{\beta}_i), & (\omega < 0) \end{cases} \quad (11)$$

where $f(\omega, \tilde{\beta}) = \{\exp(\hbar \tilde{\beta} \omega) - 1\}^{-1}$ represents the Bose-Einstein distribution. The operation φ_i^ω in Eq. (10) is given by [26]

$$\varphi_i^\omega(\rho) = \mathcal{L}_i^\omega \rho \mathcal{L}_i^{\omega\dagger} - \frac{1}{2} \{\mathcal{L}_i^{\omega\dagger} \mathcal{L}_i^\omega, \rho\}$$

where the Lindblad operators, $\{\mathcal{L}_i^\omega\}$, have the explicit forms given by

$$\begin{aligned} \mathcal{L}_1^{E_1} &= |011\rangle \langle 111| + |000\rangle \langle 100|, \\ \mathcal{L}_1^{(E_1+g)} &= (|001\rangle \langle +| - |-\rangle \langle 110|)/\sqrt{2}, \\ \mathcal{L}_1^{(E_1-g)} &= (|+\rangle \langle 110| + |001\rangle \langle -|)/\sqrt{2}, \\ \mathcal{L}_2^{E_2} &= |100\rangle \langle 110| + |001\rangle \langle 011|, \\ \mathcal{L}_2^{(E_2+g)} &= (|000\rangle \langle +| + |-\rangle \langle 111|)/\sqrt{2}, \\ \mathcal{L}_2^{(E_2-g)} &= (|+\rangle \langle 111| - |000\rangle \langle -|)/\sqrt{2}, \\ \mathcal{L}_3^{E_3} &= |110\rangle \langle 111| + |000\rangle \langle 001|, \\ \mathcal{L}_3^{(E_3+g)} &= (|100\rangle \langle +| - |-\rangle \langle 011|)/\sqrt{2}, \\ \mathcal{L}_3^{(E_3-g)} &= (|+\rangle \langle 011| + |100\rangle \langle -|)/\sqrt{2}, \end{aligned} \quad (12)$$

with $|\pm\rangle = (|010\rangle \pm |101\rangle)/\sqrt{2}$. Going to the dimensionless form, we see that the second term on the right-hand-side of Eq. (5) can be written as

$$\frac{\hbar}{k} \Phi(\rho) = \sum_{i,\omega} \gamma_i(\omega) \varphi_i^\omega(\rho), \quad (13)$$

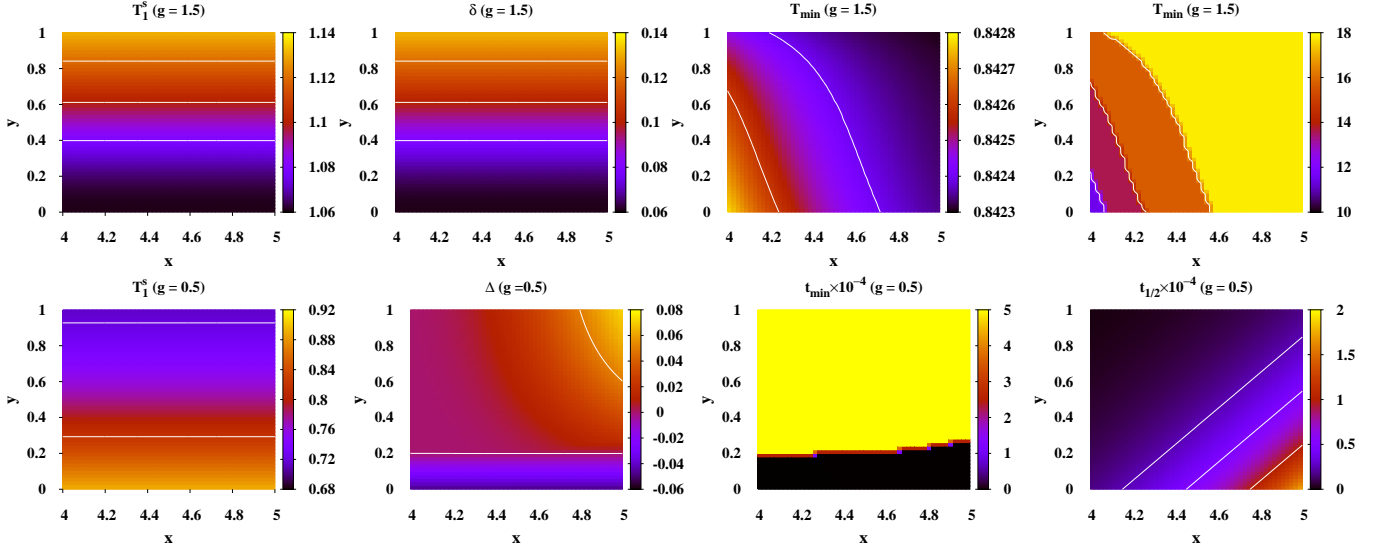


Figure 6. (Color online) System characteristics of the refrigerator modeled in Sec. II B. **Top row.** We present projection plot of (from left) T_1^s , $\delta = T_1^s - T_1$, T_{min} , and t_{min} as functions of x and y . Here, $g = 1.5$. The thin lines correspond to (from bottom to top) $T_1^s = 1.08, 1.10, 1.12$, $\delta = 0.08, 0.10, 0.12$, $T_{min} = 0.8424, 0.8426$, and $t_{min} = 12, 14, 16$. **Bottom row.** Variation of T_1^s , $\Delta = T_{min} - T_1^s$, t_{min} , and $t_{1/2}$ (from left to right) with x and y . We choose $g = 0.5$. The thin lines correspond to (from bottom to top) $T^s = 0.72$, in the case of T_1^s , $\Delta = -0.05, 0.05$, and $t_{min} = 1 \times 10^4, 5 \times 10^3, 2.5 \times 10^3$. All quantities plotted are dimensionless.

where $\gamma_i(\omega) = \frac{\hbar}{k} \gamma_i(\omega)$, and $J(\omega) = \frac{\hbar}{k} \tilde{J}(\omega)$. The transitions between a pair of eigenstates of $H_{loc} + H_{int}$, having an energy difference corresponding to ω , is governed by the operator \mathcal{L}_i^ω , while a similar operation corresponding to an energy difference of $-\omega$ is represented by $\mathcal{L}_i^{-\omega} = \mathcal{L}_i^{\omega\dagger}$. Note here that for the rotating wave approximation to be a valid one, in the present case, one has to consider a parameter space where a typical time-scale of the system is much smaller than the dissipation time, implying $\min\{E_i, g\} \gg \max\{\gamma_i\}$ [26].

Refrigeration in a necessarily transient regime and a frozen minimum temperature. To obtain the cooling only in the transient regime, CIP plays an important role to tune the qubit-bath interaction parameters, $\{\alpha_i\}$, like in the previous case. For the purpose of demonstration, we choose $x = 4$ and $y = 1$. We set the other system parameters to be $E_3 = 1$, and $T_3 = 2$, and E_2 is fixed by the equation $E_2 = E_1 + E_3$, with $E_1 = 1$ and $T_1 = 1$. The corresponding variation of $T_c(t)$ as a function of t is depicted in Fig. 5(a) for different values of g in the range $0.5 \leq g \leq 1.5$. It is clear from the figure that for a low value of g , the steady state temperature of the cold qubit may be lower than its initial temperature, T_1 . However, with increasing g , the value of T_1^s increases, and eventually crosses T_1 , thereby moving over to a region where a steady state heating of the cold qubit takes place. In this scenario, the necessity of a transient refrigeration of the cold qubit is pressing, and is obtainable at a sufficiently low time, as shown in the figure. Moreover, one should note that in the previous model, we were unable to find any range of parameters where $T_1^s > T_1$, which is observed in this model.

Let us now systematically investigate the range of (x, y) values where transient cooling is required for the three-qubit system to act as a refrigerator. We choose the region defined by

$4 \leq x \leq 5$, and $0 \leq y \leq 1$, which is justified by the validity of the quantum master equation and the form of the operator Φ (Eq. (10)). In the top row of Fig. 6, the variations of T_1^s , $\delta = T_1^s - T_1$, T_{min} , and t_{min} as functions of x and y are presented for a fixed value of $g = 1.5$. Note that the definition of δ , in the present case, corresponds to the negative of the quantity δ defined in Sec. II A, due to the possibility of heating in the steady state domain. The definitions of all the other quantities are as provided in Sec. II A. It is clear from Fig. 6 that in the entire region of the (x, y) plane considered, a steady state heating takes place, and transient cooling is the only option to use the three-qubit system as a refrigerator for the cold qubit. Similar to that in the reset model, we again determine the value of T_{min} by performing a scan over the dynamics profiles up to $t = 5 \times 10^4$. We find that for all the points in the region considered over the (x, y) plane, the cold qubit fast reaches its minimum temperature very fast, as understood from the low values of t_{min} . The maximum of t_{min} , in the region bounded by $4 \leq x \leq 5$ and $0 \leq y \leq 1$ on the (x, y) plane, is approximately 18, which is negligible compared to a typical large time required by the cold qubit to attain its steady state. Curiously, over the entire region considered, the value of T_{min} is effectively *frozen*, a variation occurring only in the fourth decimal place. This provides one the liberty to choose an appropriate set of values for x and y , when the transient refrigeration is implemented in the laboratory.

Fast and steady cooling. We conclude the discussion by mentioning the case where the possibility of fast and steady cooling exists with the low values of g . For example, consider the plots of $T_c(t)$ as functions of t for different values of g in the range $0.5 \leq g \leq 1.5$, as presented in Fig. 5(b). Here also, we consider $\alpha_1 = 10^{-(x+y)}$, $\alpha_2 = 10^{-x}$ and $\alpha_3 = 10^{-(x+y)}$ to

generate such dynamics, and we choose $x = 4$ and $y = 1$ for the purpose of demonstration. All the other system parameters are set to the same values as in the case of the transient refrigeration. We find that for low values of g , the cooling occurs considerably fast, and the steady state value is the coldest temperature attainable by the cold qubit. To investigate whether a substantial region in the parameter space can be found where such a phenomenon takes place, we focus on the same region over the (x, y) plane as discussed in the case of transient cooling, bounded by $4 \leq x \leq 5$, and $0 \leq y \leq 1$. We find that such a cooling phenomenon is present in a considerable part of our region of interest on the (x, y) -plane, as also obtained in the case of the reset model in Fig. 2 (bottom row). The variations of T_1^s , $\Delta = T_{min} - T_1^s$, t_{min} , and $t_{1/2}$, as functions of x and y are presented in the bottom row of Fig. 6, which also gives further basis to believe in the generic nature of the observation of the previous model. With increasing g , the value of the steady state temperature increases, and after a critical value, the dynamics pattern changes in such a way that the steady state temperature is no longer the minimum temperature of the cold qubit, as seen from the top row of Fig. 6 with $g = 1.5$.

III. LOW QUANTUM CORRELATIONS FAVOUR NECESSARILY TRANSIENT COOLING?

We now investigate the properties of bipartite quantum correlations, as measured by logarithmic negativity (LN) [31, 32] from the entanglement-separability domain, and quantum discord (QD) [33–35] from the information-theoretic domain, in the parameter space of the models discussed in this paper. Since the initial state of the dynamics, governed by the master equation given in Eq. (4), is a product state, both LN and QD are zero in all bipartitions for the three-qubit state at $t = 0$. As the system evolves in time, one expects generation of bipartite quantum correlations in different bipartitions of the three-qubit system at $t > 0$. This is indeed the case when LN in the case of the reset model is considered. For example, we consider the parameter values $x = 3.5$, $y = 2.5$, and plot LN against t in the bipartitions 1 : 23, 2 : 13, and 3 : 12 in Fig. 7 (left panel), keeping $g = 10^{-2}$. All the other system parameters are kept at the values as in Fig. 2. In all the bipartitions, LN increases at first, reaches a maximum, and then decreases sharply to be zero at $t \sim 200$, which is low compared to the large time scale ($\sim 5 \times 10^4$) considered in this paper. Let us denote the maximum possible value of LN in $0 \leq t \leq 500$ for the bipartition 1 : 23 by $LN_{1:23}^m$. Similarly, one can define $LN_{2:13}^m$ and $LN_{3:12}^m$ for the other two bipartitions. In the inset of Fig. 7 (left panel), we plot $LN_{1:23}^m$ as a function of x and y in the region marked by “R” in Fig. 2. The maximum value of $LN_{1:23}^m$ that is attained in the region “R” is ~ 0.016 , which is considerably low. Similar qualitative feature is found in the case of $LN_{2:13}^m$ and $LN_{3:12}^m$ in the region “R”, where the maximum values found for these two quantities are ~ 0.006 and ~ 0.014 , respectively.

Note that in major portions of the region “R”, the values of $LN_{1:23}^m$ are negligible, or zero – a feature shared by $LN_{2:13}^m$ and $LN_{3:12}^m$. Comparing $LN_{1:23}^m$ with T_{min} (comparison between

third column of Fig. 2, and inset of the left panel of Fig. 7), we find that $LN_{1:23}^m$ possesses higher values whenever T_{min} is low in comparison to the values of T_{min} in the rest of the region “R”. From the left panel of the Fig. 7, it is evident that $LN_{1:23}^m \geq LN_{2:13}^m \geq LN_{3:12}^m$. The ordering between $LN_{1:23}^m$ and $LN_{3:12}^m$ is found to remain unchanged in the entire region “R”, while that between $LN_{1:23}^m$ and $LN_{2:13}^m$ may be reversed in parts of the region “R”. The value of LN^m , in all bipartitions, decreases with decreasing g . For example, for $g = 10^{-3}$, $x = 3.5$, $y = 2.5$, and the rest of the parameters being identical to those in Fig. 2, a typical value of LN^m , in any one of the bipartitions, is of the order of 10^{-6} . Also, the area on the region “R”, where the value of LN^m is non-zero, decreases with decreasing g .

The middle panel of Fig. 7 depicts the variation of QD in all three bipartitions in the case of the reset model, with all the parameters being identical to that used in the case of LN. In all three bipartitions, QD increases with t at first, attains a maximum, and then decreases slowly with increasing t . The slow decay of QD with increasing t is in contrast with the sharp decrease of LN. Similar to LN, in the present case also, one can define QD^m corresponding to all the three bipartitions, 1 : 23, 2 : 13, and 3 : 12. In the inset of the middle panel of Fig. 7, $QD_{1:23}^m$ is plotted as a function of x and y in the region “R”, showing a qualitatively similar variation of $QD_{1:23}^m$ to that of $LN_{1:23}^m$. This feature remains unchanged for QD^m in all three bipartitions. Note also that similar to the case of LN, an ordering, given by $QD_{2:13}^m \gtrsim QD_{1:23}^m \geq QD_{3:12}^m$ is found in the case of QD in the range $0 \leq t \leq 500$. Unlike LN, this ordering remain valid over the entire region “R”. Also, for a fixed bipartition, the maximum value of QD^m found in the region “R” is higher than that corresponding to LN. Similar to the case of LN, QD^m in all the bipartitions have higher values whenever T_{min} acquires comparatively lower values in the region “R”, in the case of the reset model. Therefore, it seems that for the reset model, a low value of temperature of the cold qubit in the transient regime is related to high quantum correlations generated between different bipartitions.

In the more realistic model discussed in Sec. IIB, for all set of parameters values, (x, y) , considered in Fig. 6, no bipartite entanglement is generated in any of the bipartitions for $t > 0$. However, QD is found to be generated in all the bipartitions at $t > 0$ for a collection of values of (x, y) chosen in Fig. 6. The right panel of Fig. 7 depicts the variation of QD as a function of t in the range $0 \leq t \leq 10^3$, with $x = 4$, $y = 1$, and $g = 1.5$, for the bipartitions 1 : 23, 2 : 13, and 3 : 12. All the other parameters are set at values as in Fig. 6. The dynamics of QD in all the three bipartitions are found to be oscillatory at first. The oscillation dies out as t increases, and the system approaches towards its steady state. The maximum value of QD in all the bipartitions is reached when the steady state of the system is attained. In general, for a typical set of (x, y) values chosen in Fig. 6, the system approaches the steady state slowly, and the time taken to attain the steady state is far larger than the large time-scale considered in this paper. Due to the optimization involved in its definition, computation of QD is itself a difficult problem. Hence, determination of the variation of QD^m as a function of x and y , which involves computation of the values of QD in all three bipartitions of

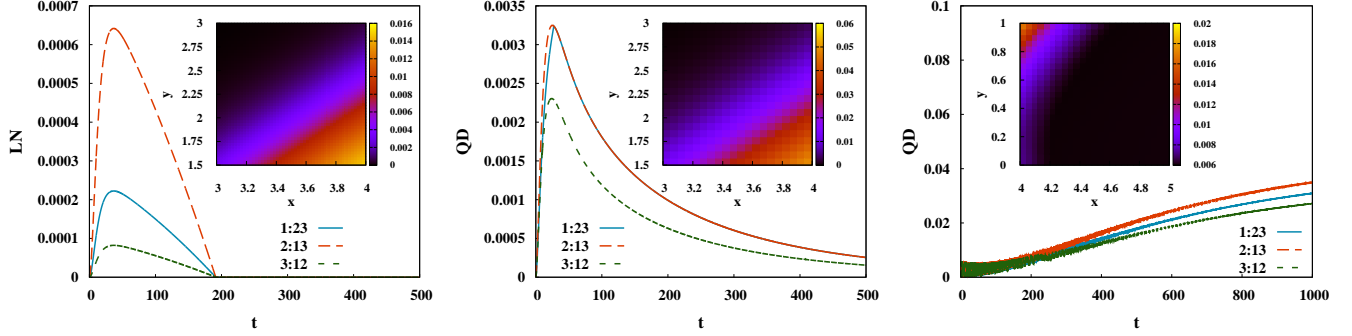


Figure 7. (Color online) Quantum correlations in refrigerator that are necessarily transient. Variation of LN (left panel), QD for reset model (middle panel), and QD for the realistic model (right panel) in the bipartitions 1 : 23 (continuous line), 2 : 13 (dashed line), and 3 : 12 (short-dashed line) as functions of t . We choose $x = 3.5$, $y = 2.5$, and $g = 10^{-2}$, while all the other parameters are fixed at the same values as in Fig. 2. (Insets) Variation of $LN_{1:23}^m$ (left panel) and $QD_{1:23}^m$ (middle panel) for the reset model, and $QD_{1:23}(t')$ as functions of x and y in the region “R” marked in Fig. 2 in the case of the realistic model. All the other parameters are fixed at the same values as in Fig. 2. All the axis plotted here are dimensionless.

the three-qubit system up to arbitrarily large time, is hard to achieve. However, when t is large, the value of QD in all three bipartitions approach their respective maximum values, QD^m , at the steady state, monotonically with increasing t . Let us denote the value of QD in the bipartition 1 : 23 and at a specific time $t = t'$ by $QD_{1:23}(t')$. With the above observations in mind, we expect the qualitative features of the variations of $QD_{1:23}^m$ with x and y to be similar to that of $QD_{1:23}(t')$, where t' can be chosen to be a physically tractable time.

We choose $t' = 10^3$, and the variation of $QD_{1:23}(10^3)$, as a function of x and y , is represented in the inset of Fig. 7 (middle panel), where $g = 1.5$, and similar range of (x, y) values, as presented in Fig. 6, are chosen. The other parameter values are kept fixed at values as in Fig. 6. We observe that high values of $QD_{1:23}(10^3)$ are found when x is low, and y is high. This feature remains qualitatively similar in the case of all three bipartitions. Interestingly, when the value of g is decreased, higher values of QD at $t = 10^3$ for all the three bipartitions are found for high values of x and low values of y . Note here that the steady state heating phenomena is observed with increasing values of g . This implies that for fixed values of the parameters (x, y) , steady state heating with increasing g is associated with an increase in the values of $QD(10^3)$ in any one of the bipartitions. Note also that although TC is the only option in the entire region on the (x, y) -plane considered in Fig. 6, for $g = 1.5$, lower values of T_{min} is found in regions where values of both x and y are high. However, in those regions, the value of $QD_{1:23}(10^3)$ is negligible, or zero, as can be clearly seen from Fig. 7 (inset of right panel). This is in contrast to the findings in the case of LN, when reset model is considered.

The above results motivate one to conclude that in the situations where parameter values are chosen according to CIP, occurrence of TC without SSC is always associated with a complete absence, or a very low value of bipartite quantum correlations in the time evolved states of the three-qubit system. It has been shown that entanglement can enhance SSC in three-qubit systems modeled by the reset model [23]. Our findings, on the

other hand, suggest that to find TC without SSC, generation of three-qubit states with very low, or no bipartite entanglement is necessary. Also, our results lead us to consider this feature to be a generic one for the three-qubit absorption refrigerator, irrespective of the type of baths.

IV. CONCLUSION

In conclusion, we study the three-qubit self-contained quantum absorption refrigerator in the transient regime. We obtain ranges of parameters of the system’s dynamics where it is necessary to consider refrigeration in the transient regime. We propose a canonical form of the qubit-bath interaction parameters that facilitates the consideration of such a transient refrigeration without steady state cooling. More specifically, we consider two different models of thermalization for the three-qubit absorption refrigerator, where the dynamics of the system is governed by the quantum master equation under Born-Markov approximation. We show that following our canonical form of the interaction parameters, there exist situations where the cooling of the cold qubit is possible only in the transient regime, while the steady state does not provide any advantage regarding cooling. In a realistic scenario, where the local heat-baths are modeled by infinite collections of harmonic oscillators, and the qubit-bath interactions are defined by ohmic spectral functions, we demonstrate that a steady state heating is possible, which emphasizes the necessity of transient cooling in order to obtain refrigeration. We also show that in the space of the system parameters and the parameters defining the qubit-bath interactions, there exists substantial regions where transient cooling without the steady state cooling takes place. Moreover, with a modified canonical form of the qubit-bath interaction parameters, we show that a fast cooling of the cold qubit is also possible, where the coldest temperature is attained at the steady state. Our study indicates that the transient cooling without a steady state cooling may be a generic phenomena in all thermalization models, where the dynamics of the system

is governed by quantum master equations. We also show that the occurrence of transient cooling without a steady state cooling is associated with the generation of negligible, or no bipartite quantum correlations in all the bipartitions of the time-evolved three-qubit state. We find that the system for which the

thermalization process is modeled by heat baths consisting of an infinite number of oscillators, there appears a phenomenon of freezing of the minimum attainable temperature of the cold qubit with respect to change in system parameters.

-
- [1] G. Gemma, M. Michel, and G. Mahler, *Quantum Thermodynamics* (Springer, New York, 2004).
 - [2] E. P. Gyftopoulos and G. P. Beretta, *Thermodynamics: Foundations and Applications* (Dover, New York, 2005).
 - [3] D. Janzing, P. Wocjan, R. Zeier, R. Geiss, and T. Beth, *Int. J. Theor. Phys.* **39**, 2717 (2000).
 - [4] A. E. Allahverdyan and Th. M. Nieuwenhuizen, *Phys. Rev. Lett.* **85**, 1799 (2000).
 - [5] F. Tonner and G. Mahler, *Phys. Rev. E* **72**, 066118 (2005); M. Henrich, M. Michel, and G. Mahler, *Europhys. Lett.* **76**, 1057 (2006); F. Rempp, M. Michel, and G. Mahler, *Phys. Rev. A* **76**, 032325 (2007); M. J. Henrich, G. Mahler, and M. Michel, *Phys. Rev. E* **75**, 051118 (2007); M. Perarnau-Llobet, K. V. Hovhannisyan, M. Huber, P. Skrzypczyk, N. Brunner, and A. Acín, *Phys. Rev. X* **5**, 041011 (2015); M. Huber, M. Perarnau-Llobet, K. V. Hovhannisyan, P. Skrzypczyk, C. Klöckl, N. Brunner, and A. Acín, *New J. Phys.* **17**, 065008 (2015); M. Navascués and L. P. García-Pintos, *Phys. Rev. Lett.* **115**, 010405 (2015); A. Misra, U. Singh, S. Bhattacharya, and A. K. Pati, *Phys. Rev. A* **93**, 052335 (2016).
 - [6] R. Alicki and M. Fannes, *Phys. Rev. E* **87**, 042123 (2013).
 - [7] F. Brandao, M. Horodecki, N. Ng, J. Oppenheim, and S. Wehner, *Proc. Natl. Acad. Sci. U.S.A.* **112**, 3275 (2015); M. Lostaglio, D. Jennings, and T. Rudolph, *Nature Commun.* **6**, 6383 (2015).
 - [8] R. Uzdin, A. Levy, and R. Kosloff, *Phys. Rev. X* **5**, 031044 (2015) and references therein.
 - [9] E. Geva and R. Kosloff, *J. Chem. Phys.* **96**, 3054 (1992); E. Geva and R. Kosloff, *J. Chem. Phys.* **104**, 7681 (1996); T. Feldmann and R. Kosloff, *Phys. Rev. E* **61**, 4774 (2000); J. P. Palao, R. Kosloff, and J. M. Gordon, *Phys. Rev. E* **64**, 056130 (2001).
 - [10] D. Segal and A. Nitzan, *Phys. Rev. E* **73**, 026109 (2006).
 - [11] T. Feldmann, E. Geva, and P. Salamon, *Am. J. Phys.* **64**, 485 (1996); T. Feldmann and R. Kosloff, *Phys. Rev. E* **68**, 016101 (2003); R. Kosloff and T. Feldmann, *Phys. Rev. E* **82**, 011134 (2010).
 - [12] H. T. Quan, Y.-X. Liu, C. P. Sun, and F. Nori, *Phys. Rev. E* **76**, 031105 (2007).
 - [13] G. P. Beretta, arXiv:0703.3261 [quant-ph] (2007).
 - [14] F. Giazotto, T. T. Heikkilä, A. Luukanen, A. M. Savin, and J. P. Pekola, *Rev. Mod. Phys.* **78**, 217 (2006).
 - [15] Y.-X. Chen and S.-W. Li, *Europhys. Lett.* **97**, 40003 (2012).
 - [16] D. Venturelli, R. Fazio, and V. Giovannetti, *Phys. Rev. Lett.* **110**, 256801 (2013).
 - [17] O. Abah, J. Roßnagel, G. Jacob, S. Deffner, F. Schmidt-Kaler, K. Singer, and E. Lutz, *Phys. Rev. Lett.* **109**, 203006 (2012).
 - [18] J. P. Palao, R. Kosloff, and J. M. Gordon, *Phys. Rev. E* **64**, 056130 (2001); S. Popescu, A. J. Short, and A. Winter, *Nat. Phys.* **2**, 754 (2006); Y. Zhou and D. Segal, *Phys. Rev. E* **82**, 011120 (2010); A. Levy, R. Alicki, and R. Kosloff, *Phys. Rev. E* **85**, 061126 (2012); R. Dorner, J. Goold, C. Cormick, M. Paternostro, and V. Vedral, *Phys. Rev. Lett.* **109**, 160601 (2012); A. Levy and R. Kosloff, *Phys. Rev. Lett.* **108**, 070604 (2012); D. Egloff, O. C. O. Dahlsten, R. Renner, and V. Vedral, *New J. Phys.* **17**, 073001 (2015); R. Kosloff and A. Levy, *Annu. Rev. Phys. Chem.* **65**, 365 (2014); D. Gelbwaser-klimovsky, W. Niedenzu, and G. Kurizki, *Adv. At. Mol. Opt. Phys.* **64**, 329 (2015); J. Goold, M. Huber, A. Riera, L. del Rio, and P. Skrzypczyk, arXiv:1505.07835 [quant-ph] (2015); S. Vinjanampathy and J. Anders, arXiv:1508.06099 [quant-ph] (2015).
 - [19] F. Curzon and B. Ahlborn, *Am. J. Phys.* **43**, 22 (1975); S. Velasco, J. M. M. Roco, A. Medina, and A. C. Hernández, *Phys. Rev. Lett.* **78**, 3241 (1997); M. Esposito, R. Kawai, K. Lindenberg, and C. Van den Broeck, *Phys. Rev. Lett.* **105**, 150603 (2010); A. E. Allahverdyan, K. Hovhannisyan, and G. Mahler, *Phys. Rev. E* **81**, 051129 (2010); Y. Wang, M. Li, Z. C. Tu, A. C. Hernández, and J. M. M. Roco, *Phys. Rev. E* **86**, 011127 (2012); A. Misra, U. Singh, M. N. Bera, and A. K. Rajagopal, *Phys. Rev. E* **92**, 042161 (2015); B. Gardas and S. Deffner, *Phys. Rev. E* **92**, 042126 (2015).
 - [20] N. Linden, S. Popescu, and P. Skrzypczyk, *Phys. Rev. Lett.* **105**, 130401 (2010).
 - [21] P. Skrzypczyk, N. Brunner, N. Linden, and S. Popescu, *J. Phys. A: Math. Theor.* **44**, 492002 (2011).
 - [22] N. Brunner, N. Linden, S. Popescu, and P. Skrzypczyk, *Phys. Rev. E* **85**, 051117 (2012).
 - [23] N. Brunner, M. Huber, N. Linden, S. Popescu, R. Silva, and P. Skrzypczyk, *Phys. Rev. E* **89**, 032115 (2014).
 - [24] J. B. Brask and N. Brunner, *Phys. Rev. E* **92**, 062101 (2015).
 - [25] L. A. Correa, J. P. Palao, G. Adesso and D. Alonso, *Phys. Rev. E* **87**, 042131 (2013).
 - [26] M. T. Mitchison, M. P. Woods, J. Prior and M. Huber, *New J. Phys.* **17**, 115013 (2015).
 - [27] A.R. Calderbank, P.W. Shor, *Phys. Rev. A* **54**, 1098 (1996).
 - [28] Y.-X. Chen and S.-W. Li, *Europhys. Lett.* **97**, 40003 (2012); D. Venturelli, R. Fazio, and V. Giovannetti, *Phys. Rev. Lett.* **110**, 256801 (2013).
 - [29] R. Landauer, *IBM J. Res. Dev.* **5**, 183 (1961); C. H. Bennett, *Int. J. Theor. Phys.* **21**, 905 (1982).
 - [30] H. Breuer and F. Petruccione, *The Theory of Open Quantum Systems* (Oxford University Press, New York, 2002).
 - [31] The logarithmic negativity (LN) [32] of a bipartite quantum state ρ_{AB} is defined as $LN(\rho_{AB}) = \log_2[2N(\rho_{AB}) + 1]$, where $N(\rho_{AB}) = (\|\rho_{AB}^{T_A}\|_1 - 1)/2$ is the negativity of ρ_{AB} , defined as the absolute value of the sum of all the negative eigenvalues of $\rho_{AB}^{T_A}$. Here, $\rho_{AB}^{T_A}$ is the partially transposed form of ρ_{AB} with respect to the subsystem A , and $\|\rho\|_1 \equiv \text{tr}\sqrt{\rho^\dagger\rho}$ is the trace-norm of the matrix ρ .
 - [32] A. Peres, *Phys. Rev. Lett.* **77**, 1413 (1996); M. Horodecki, P. Horodecki, and R. Horodecki, *Phys. Lett. A* **223**, 1 (1996); K. Życzkowski, P. Horodecki, A. Sanpera, and M. Lewenstein, *Phys. Rev. A* **58**, 883 (1998).
 - [33] The quantum discord (QD) [35], $QD(\rho_{AB}) = \mathcal{I}(\rho_{AB}) - \mathcal{J}(\rho_{AB})$, of a bipartite quantum state ρ_{AB} , is defined as the minimum difference between the total correlation [34] $\mathcal{I}(\rho_{AB}) = S(\rho_A) + S(\rho_B) - S(\rho_{AB})$, quantified by the quantum mutual information, and the classical correlation, $\mathcal{J}(\rho_{AB}) = S(\rho_B) - S(\rho_{B|A})$, present in the system. Here, $\rho_{A(B)} = \text{tr}_{B(A)}[\rho_{AB}]$ are

the local density matrices of ρ_{AB} , $S(\varrho) = -\text{tr}(\varrho \log_2 \varrho)$ is the von Neumann entropy, and $S(\rho_{B|A}) = \min_{\{P_i\}} \sum_i p_i S(\rho_{B|i})$ is the conditional entropy, conditioned over the measurements performed on A via a rank-one projective measurements $\{P_i\}$, which produces the states $\rho_{B|i} = \frac{1}{p_i} \text{tr}_A[(P_i \otimes \mathbb{I}_B) \rho_{AB} (P_i \otimes \mathbb{I}_B)]$, with probabilities $p_i = \text{tr}[(P_i \otimes \mathbb{I}_B) \rho_{AB} (P_i \otimes \mathbb{I}_B)]$. The identity operator in the Hilbert space of B is denoted by \mathbb{I}_B .

- [34] W. H. Zurek, in Quantum Optics, Experimental Gravitation and Measurement Theory, edited by P. Meystre and M. O. Scully (Plenum, New York, 1983); S. M. Barnett and S. J. D. Phoenix, Phys. Rev. A **40**, 2404 (1989). B. Schumacher and M. A. Nielsen, Phys. Rev. A **54**, 2629 (1996); N. J. Cerf and C. Adami, Phys. Rev. Lett. **79**, 5194 (1997); B. Groisman, S. Popescu, and A. Winter, ibid. **72**, 032317 (2005).
- [35] L. Henderson and V. Vedral, J. Phys. A: Math. Gen. **34**, 6899 (2001); H. Ollivier and W. H. Zurek, Phys. Rev. Lett. **88**, 017901 (2001).